MATERIALS CHEMISTRY
FRONTIERS

RESEARCH ARTICLE

View Article Online
View Journal | View Issue

Cite this: *Mater. Chem. Front.*, 2023, **7**, 267

Solution-processed triphenylethylene-fluorene fluorochromes toward deep-blue organic light-emitting diodes: benefits of preventing radical formation†

Yingying Zheng,‡[a] Mengyuan Li,‡[a] Ninging Yu,‡[a] Shengjie Wang,[a] Lili Sun,[a] Xiang An,[a] Yamin Han,[a] Jinyi Lin,[a] *[a] Xuehua Ding*[a] and Wei Huang*[abc]

High band exciton is easily trapped and quenched by the defect structure in wide bandgap light-emitting conjugated materials (LCMs), which is harmful to the performance and stability of deep-blue organic light-emitting diodes (OLEDs). In fact, an unsaturated aromatic unit is an unstable segment that is easily attacked by external influence to form organic radical, which may cause a complicated photophysical property that reduce the efficiency and stability of OLEDs. Herein, two triphenylethylene-fluorene LCMs (F-TrPE-MC_8 and M-TrPE-MC_8) are obtained with an efficient deep-blue emission toward deep-blue OLEDs. First, two materials present deep-blue emission with high efficiency of nearly 80% in the solid state, which is associated with their intramolecular singlet exciton behavior, according to time-resolved transient spectroscopy. However, unsaturated double bonds are easily activated by the synergistic effect of light and oxygen, resulting in the formation of organic radicals in solid films. These organic radicals may trap and quench the singlet exciton and further cause relatively low emission efficiency. Finally, compared to the device based on the aged film under light excitation, OLEDs based on pristine spin-coated films exhibited a better device performance and more stable deep-blue emission (0.16, 0.09), confirming the importance of the suppression of organic radicals in LCMs.

Received 13th October 2022,
Accepted 29th November 2022

DOI: 10.1039/d2qm01053d

rsc.li/frontiers-materials

Introduction

Solution-processed organic light-emitting conjugated materials (LCMs) are widely applied in the information display, solid light and organic lasers owing to their easily structural modification, low-cost device fabrication, and potentially mechanical flexibility.[1–6] In fact, compared to the red and green ones, deep-blue LCMs always present a wide bandgap, low charge density and charge mobility, which may be easily doped with a trapped defect structure.[7–12] Therefore, compared to green and red ones, deep-blue organic light-emitting diodes (OLEDs) show a relatively low stability of colour purity, low efficiency and short operation lifetime.[3,7,12–16] To date, the reasons to cause their instability and low efficiency are divided into intrinsic and external mechanisms.[17–19] The former one is attributed to the multi-exciton coupling/annihilation, charge carrier accumulation, and changes under the electric field, and the latter one involved high-band light, oxygen, water, heat, temperature, and current density.[20,21] The penetration of oxygen atoms may result in the oxidation of organic aromatic units, the defect traps of carriers and excitons, and photoinduced degradation reactions.[7,17,22,23] Among all factors, organic radicals, especially σ-types, act as unstable and active centres, which may form a relatively stabilized delocalized π-radicals and complex mixture of degradation products under electrical field.[16,24,25] It is reasonably foreseen that these defect radicals will act as deep centres to trap exciton.[26–29] All these unexpected parameters induced by external parameters, such as light, oxygen, and water, result in the instability and degradation of deep-blue OLEDs.[16,25,30] Therefore, to systematically explore the effect of organic radicals on the photophysical processing in deep-blue LCMs, which are preconditions to fabricate stable and efficient deep-blue OLEDs.

In general, conjugated aromatic units along backbone structures enable chain to show long-range π-electron delocalization,

[a] *Key Laboratory of Flexible Electronics (KLoFE) and Institute of Advanced Materials (IAM) Nanjing Tech University (Nanjing Tech), 30 South Puzhu Road, Nanjing 211816, China. E-mail: iamjylin@njtech.edu.cn, iamxhding@njtech.edu.cn wei-huang@njtech.edu.cn*
[b] *State Key Laboratory of Organic Electronics and Information Displays & Institute of Advanced Materials (IAM), Nanjing University of Posts & Telecommunications, 9 Wenyuan Road, Nanjing 210023, China*
[c] *Frontiers Science Center for Flexible Electronics & Institute of Flexible Electronics (IFE) Northwestern Polytechnical University (NPU), Xi'an 710072, China*

† Electronic supplementary information (ESI) available. See DOI: https://doi.org/10.1039/d2qm01053d

‡ Yingying Zheng, Mengyuan Li and Ninging Yu are contributed equally to this work.

which is the origin of optoelectronic property of organic conjugated materials.[31] These aromatic systems easily react by external parameters to cause the formation of delocalized π-radicals.[16,24] In particular, compared to non-polaron hydrocarbons, a high π-electron delocalization of p (donor)–n (acceptor) conjugated molecules always presents an excellent electronic landscape to be attacked by external reactive intermediate species (such as ionic and radical),[27,28] which cause the formation of defect structure and trapped sites and centre, resulting in low emission stability and efficiency.[23,27,32] In fact, unsaturated double bond is a defect site in conjugated molecules,[22] which are easily attacked by the external parameters, such as light, water, and oxygen, although they are stabilized by the conjugated molecular framework.[16,18,26] Herein, we introduce a steric unsaturated double bond contained units, triphenylethylene,[33] to systematically explore the effect of the formation of organic radicals on the photophysical processing of deep-blue LCMs toward stable and deep-blue OLEDs. First, two solution-processed triphenylethylene-fluorene fluorochromes (F-TrPE-MC_8 and M-TrPE-MC_8) were designed and prepared with an extremely efficient deep-blue emission. Corresponding spin-coated films had high photoluminance quantum efficiency (PLQE) of nearly to 80% owing to their single-molecular excitonic behavior.[7,15] As we expected, organic radicals were formed under light excitation in the air.[16,18] Moreover, both OLEDs based on two type pristine films showed a stable deep-blue emission with a CIE of (0.16, 0.09) but changed to the unstable sky-blue emission after the formation of organic radical. Interestingly, compared with the radical-contained films, both OLEDs based on the pristine films displayed a better and more stable color purity of deep-blue emission.

Results and discussion

The synthetic routes and chemical structures of these triphenylethylene-fluorene fluorochromes (F-TrPE-MC_8 and M-TrPE-MC_8) are illustrated in Scheme S1 (ESI†). These two novel derivatives are prepared by Witting reaction,[34,35] and the boronic acid esters of diarylfluorenes are synthesized based on previous studies.[36–38] The aimed molecules F-TrPE-MC_8/M-TrPE-MC_8 are prepared by Suzuki coupling reaction. Their chemical structures were confirmed by ^{1}H NMR, ^{13}C NMR spectral analysis and high-resolution mass spectroscopy (Fig. S1–S6, ESI†). Additionally, both compounds had high decomposition temperatures (T_d) of 400 °C determined by thermogravimetric analysis (TGA) (Fig. S7a, ESI†). The glass transition temperatures (T_g) of both compounds exceed 100 °C measured by differential scanning calorimetry (DSC) (Fig. S7b, ESI†). Simultaneously, two materials exhibit excellent solubility in some common organic solvent, such as toluene, dichloromethane, trichloromethane and acetonitrile. Cyclic voltammetry (CV) analysis illustrates that the highest occupied molecular orbital (HOMO) and the lowest unoccupied molecular orbital (LUMO) energy levels of F-TrPE-MC_8 and M-TrPE-MC_8 are estimated at about −5.65 eV, −5.63 eV, and −2.22 eV, −2.31 eV, respectively (Fig. S8, ESI†).

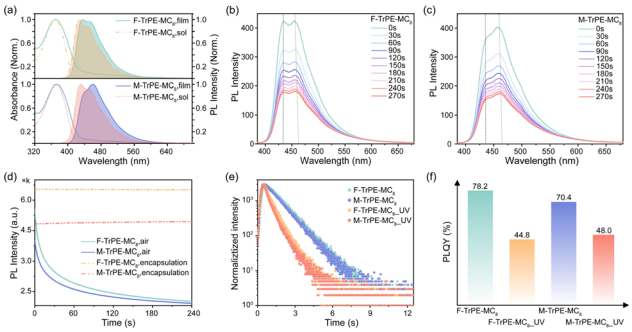

Fig. 1 Optical property of F-TrPE-MC_8 and M-TrPE-MC_8 in various states. (a) Absorption and PL spectra of F-TrPE-MC_8 and M-TrPE-MC_8 in dilute solution and film. Time-dependent PL spectra of F-TrPE-MC_8_UV (b) and M-TrPE-MC_8_UV (c) films upon ultraviolet excitation under air atmosphere. The emission intensity of the two films declined slowly, prolonging the time of light excitation. Time-dependent emission intensity of F-TrPE-MC_8 and M-TrPE-MC_8 (d) films upon ultraviolet excitation under air and N_2 atmosphere. Decay time (e) and PLQY (f) of F-TrPE-MC_8 and M-TrPE-MC_8 pristine and aged films. Singlet exciton is easily quenched and trapped by the organic radicals, which may cause a shorter decay time and emission efficiency.

Subsequently, we further investigated the optical properties of F-TrPE-MC_8 and M-TrPE-MC_8 in solution and films. As shown in Fig. 1a, two materials displayed two similar absorption peaks at 370 nm and 373.5 nm in dilute solution and spin-coating film, respectively, attributed to the π–π* transitions of conjugated backbone structures.[33] Moreover, the corresponding PL spectra consisted of two similar peaks at 430 nm and 450 nm, respectively. Interestingly, for the F-TrPE-MC_8, the similar emission spectral profile with two peaks at 435.6 nm (0–0) and 454.2 nm (0–1) in dilute solution and film effectively confirmed the single-molecular excitonic behaviour. Compared to the solution state, the slightly red-shifted (4 nm) emission spectra of the spin-coated films were assigned to the restriction of the conformational motion in solid states.[39] Additionally, for M-TrPE-MC_8, it shows a red-shift compared film to solution and a distinct change of spectral profile. The emission intensity of the M-TrPE-MC_8 film at 460.6 nm (0–1) was slightly stronger than that at 441 nm (0–0), attributed to the appearance of weak intermolecular aggregation or charge-transfer interaction. Moreover, M-TrPE-MC_8 has a slight red-shift against F-TrPE-MC_8 in both film and solution owing to the weak electron-withdrawing ability of methyl group compared with fluorine ones.[31] The fluorescence lifetimes (τ) of the two compounds in film were further studied by time-resolved transient PL analysis (Fig. 1e and Table 1). The lifetime decays for both types of emissions exhibited a single-exponential character, with an averaged lifetime (τ) of about 1.14 ns for F-TrPE-MC_8 and 1.10 ns for M-TrPE-MC_8. High fluorescence quantum efficiency (Φ) of 78.2% and 70.4% are observed for the F-TrPE-MC_8 and M-TrPE-MC_8 spin-coated films, respectively, owing to the π–π* transition ascribed to the high degree of conjugation and molecular rigidity. Thus, the radiative decay rate ($K_r = \phi/\tau$) of F-TrPE-MC_8 and M-TrPE-MC_8 is calculated for 6.86×10^8 s^{-1} and 6.40×10^8 s^{-1}. All the results of spin-coating films above was obtained with the films encapsulated by a cover glass to isolate the oxygen.

Table 1 Photophysical property of two novel materials

Materials	λ_{ab} (nm)	λ_{em} (nm)	λ_{ex} (nm)	ϕ_F (%)	τ_{FL} (ns)	K_r (s^{-1})	K_{nr} (s^{-1})
F-TrPE-MC_8	370	435/454	368	78.2	1.14	6.86×10^8	1.91×10^8
F-TrPE-MC_8-UV	370	435/454	368	44.8	0.64	7.00×10^8	8.63×10^8
M-TrPE-MC_8	373	441/460	364	70.4	1.10	6.40×10^8	2.69×10^8
M-TrPE-MC_8-UV	373	441/460	364	48.0	0.57	8.42×10^8	9.12×10^8

More interestingly, if we kept the spin-coating films (recorded as F-TrPE-MC_8_UV and M-TrPE-MC_8_UV) in ultraviolet excitation under air atmosphere, the lifetime and PLQY are reduced rapidly. The emission spectra of the two compounds for spin-coated films were collected at intervals of 30 s because the films were exposed in air, which indicates that there were no slight shift in the emission spectra but reduced the emission intensity (Fig. 1b and c). Time-dependent emission intensity curves of the two films exposed air are provided to screen the decrease in emission efficiency concisely and clearly (Fig. 1d). There is no obvious change in the emission intensity if we kept sample in the N_2 atmosphere under ultraviolet excitation, suggesting the synergistic effect of light excitation and O_2. To confirm this assumption, we added the 25% (weight ratio) of DMPO into F-TrPE-MC_8/M-TrPE-MC_8 toluene solution (10 mg mL^{-1}) to trap radical. As we expected, both F-TrPE-MC_8 and M-TrPE-MC_8/DMPO mixed films exhibited similar emission intensity after ultraviolet excitation in the air compared to the pristine ones (Fig. 2a). However, their lifetimes (τ) at 0–0 band emission are reduced to 0.71 ns and 0.65 ns, respectively. The addition of DMPO can efficiently restrict the change tendency in emission efficiency. Subsequently, to deeply explore the effect mechanism of the O_2, two possible routes must be considered, as shown in Scheme 1b, such as material decomposition and organic radical. Therefore, MALDI-TOF MS analysis is first explored here to check the mechanism of material decomposition. Owing to MALDI-TOF MS curves (Fig. 2b), no new substances with low molecular weights are observed after ultraviolet oxygen treatment. Additionally, as displayed in the ^1H NMR spectra after light excitation (Fig. S12 and S13, ESI†), beyond the parent one, there is no extra signal peak observed, indicating that no new product is formed, which agree with the MALDI-TOF MS results. Therefore, we can exclude the possibility that excimer or ring-closure reactions occur between the unsaturated double bond of triphenylethylene moieties or the decomposition of material among the fluorescence quenching process under the effect of light and oxygen.[16,18,27] Then, electron paramagnetic resonance (EPR) technique applied to check the organic radicals emerge in the photoluminescence process. 5,5-Dimethyl-1-pyrroline *N*-oxide (DMPO) is a kind of radical scavenger applied to the electron paramagnetic resonance (EPR) technique to trap some radicals.[40] We tested the radicals of the two materials in diluted solutions, such as aerated nitrogen atmosphere, nitrogen with ultraviolet irradiation condition, aerated air condition (Fig. S14 and S15, ESI†), and the presence of air with ultraviolet irradiation condition. Finally, in an air atmosphere, the signal was detected in the sample exposed to ultraviolet irradiation for the solution containing DMPO. To confirm the type of radical, a full EPR spectrum of DMPO-adduct was recorded (Fig. 2c). The adduct of DMPO with singlet oxygen, abbreviated as DMPO-$^1O_2$, has 3 signal peaks, from left to right, and 3 equal heights, 1 : 1 : 1.[41–43] As shown in Fig. 2c, the last signal is lower than the first two because the

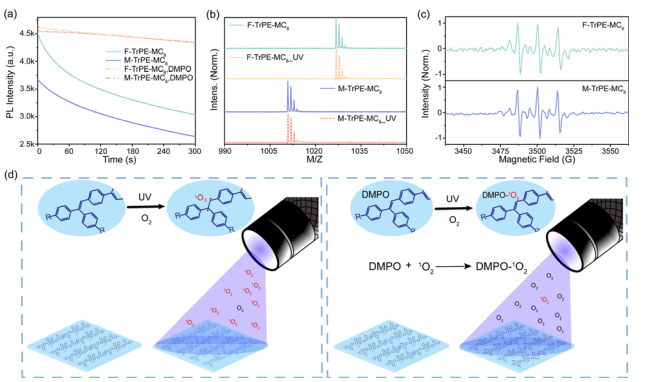

Fig. 2 Mechanism investigation of the exciton quenching in the F-TrPE-MC_8_UV and M-TrPE-MC_8_UV films. (a) Time-dependent emission intensity of pristine F-TrPE-MC_8 and M-TrPE-MC_8, F-TrPE-MC_8 and M-TrPE-MC_8/DMPO mixed films (a) upon ultraviolet excitation under air atmosphere. (b) Maldi-Tof data of F-TrPE-MC_8 and M-TrPE-MC_8 samples after ultraviolet excitation under air atmosphere. (c) EPR curves of F-TrPE-MC_8 and M-TrPE-MC_8 mixed with DMPO. (d) Possible mechanism of the formation of organic radical in F-TrPE-MC_8 and M-TrPE-MC_8.

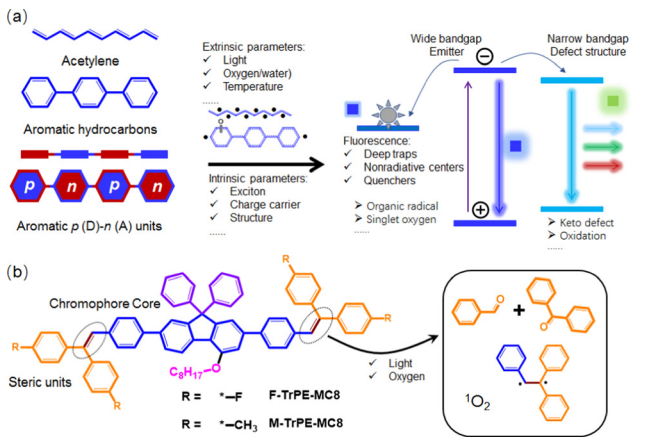

Scheme 1 (a) Schematic illustration of organic radical in conjugated molecules. Organic radicals, included stable and unstable ones, are caused by the intrinsic and extrinsic factors, which may induce a complicated photophysical behavior in solid states.[27,28,31] (b) Chemical structures of our model deep-blue LCMs (F-TrPE-MC_8 and M-TrPE-MC_8) with an unsaturated double bonds. Unsaturated double bonds in LCMs are easily attacked by the light and oxygen, resulting in the material decomposition[17,22] and formation of organic radical,[18,24] which may significantly affect the optical property of LCMs in solid states.[16,18]

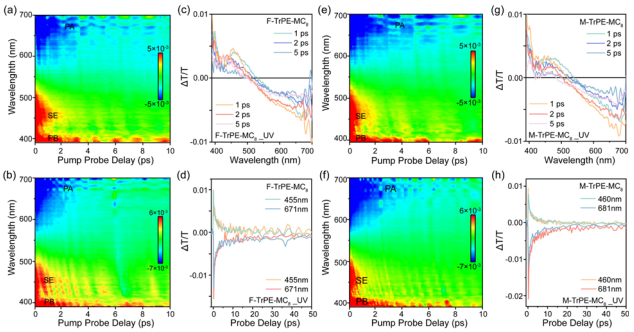

Fig. 3 $\Delta T/T$ kinetics of transient absorption spectra of F-TrPE-MC_8 and M-TrPE-MC_8 in solid states. The 2D contour plot of TA spectra in F-TrPE-MC_8 (a), F-TrPE-MC_8_UV (b), M-TrPE-MC_8 (e) and M-TrPE-MC_8_UV (f) encapsulated films, respectively. (c and g) Spectra of films before and after ultraviolet radiation at different probe delay times. (d and h) The comparison of SE time-decay dynamics at the selected wavelength of films and the PA dynamics tracing.

solution is blocked. The ESR parameters coincided with those of the DMPO-$^1O_2$ adduct and strongly supported the triple signal DMPO-$^1O_2$ adduct. Singlet oxygen is a kind of reactive oxygen without paramagnetism, which is the excited state of ordinary oxygen ($^3O_2$). Based on the above analysis, we conclude that $^1O_2$ was formed by $^3O_2$ under the combined action of total environmental effects. According to the results above, a reasonable inference was drawn from the outcome. The radicals generated during the photoluminescence process with the combined action of ultraviolet and oxygen, with the specific process is shown in Fig. 2d.[16,18,27] We estimate that the entire system condition induces the generation of $^1O_2$. Moreover, the double bond of triphenylethylene may be attacked by the $^1O_2$ radicals because the unsaturated double bond becomes unstable. The addition of 25% content DMPO captures $^1O_2$, making further efforts to impede the radical formation. Ultimately, fluorescence roll-off is effectively suppressed. Thus, the formation of organic radicals can easily reduce the emission efficiency and color purity in the films, which is detrimental to the fabrication of OLEDs.

In general, femtosecond transient absorption (fs-TA) is an effective tool to explore the excitonic behavior in the solid states.[7,44] Therefore, fs-TA analyses of F-TrPE-MC_8 and M-TrPE-MC_8 films are introduced here to investigate their ultrafast photoexcitation dynamics behavior (Fig. 3). The 2D contour plot of TA spectra in F-TrPE-MC_8 and F-TrPE-MC_8_UV films (both films were encapsulated by cover glasses through the measurement process) demonstrates an obvious stimulated radiation (SE, $\Delta T/T > 0$) signal accompanied with a photo-induced bleach (PB, $\Delta T/T > 0$) signal and a photoinduced absorption (PA, $\Delta T/T < 0$) signal in the initial time (Fig. 3a and b). Then, transmission ($\Delta T/T$) spectra at 1, 2, and 5 ps delay time of the two films are depicted in Fig. 3c and d. Their $\Delta T/T$ spectra are composed of a strong PB band below 420 nm, a SE band at 420–490 nm, and a PA band estimated at 550–700 nm. In addition, the SE-to-PA zero-crossing point shows a blueshift with a delay prolong of their respective process with a delay prolong. Interestingly, strong SE band also revealed their robust deep-blue emission, reasonably explaining their extremely high PLQY (up to nearly 80%). Compared to the delay prolong of pristine film, the junction of PA signal and SE signal changed to the direction of short band in the aged film, indicating the rapid single exciton decay that consisted of the shorter lifetime above. Moreover, the weak SE and strong PA band also caused the low deep-blue emission efficiency after the formation of organic radicals. More importantly, symmetric $\Delta T/T$ curves of SE time-decay dynamics (455 nm) and PA dynamics tracing (671 nm) also confirmed the deep-blue emission from singlet excitons but no influence from polaron pairs (Fig. 3d).[7] Compared to pristine films, slightly weak SE band was found for the M-TrPE-MC_8 and M-TrPE-MC_8_UV film, associated with the exciton quenching upon the formation of organic radical, resulting in the formation of an undesirable polaron pair. Their single excitons decayed rapidly, supporting that the excitons are quenched by organic radicals and reduced the emission efficiency. Although it is not unique, there are strong intensities at the polaron band between 550 and 700 nm, which also effectively supports the observation above. Interestingly, similar to pristine ones, as illustrated in Fig. 3h, there is extremely perfect symmetry $\Delta T/T$ behaviour of the dynamic of SE and PA owing to the intramolecular emission behaviour without any other emissive species. Therefore, these results above effectively concluded that the formation of organic radicals in our materials can quench exciton, reducing emission efficiency and stability.

To check the effect of organic radical on electroluminescene (EL) properties, preliminary OLEDs are fabricated with a conventional structure. First, film morphology of two pristine and aged (UV light excitation) F-TrPE-MC_8 and M-TrPE-MC_8 spin-coated films was analysed by performing atomic force microscopy (AFM) analysis. As depicted in Fig. S16, all F-TrPE-MC_8, M-TrPE-MC_8, F-TrPE-MC_8_UV and M-TrPE-MC_8_UV films exhibited a smooth and continuous surface morphology with a root mean square (RMS) roughness of 0.209, 0.235, 0.293 and 0.357 nm, respectively. Then, device performances are illustrated in Fig. 4. First, for the OLEDs based on F-TrPE-MC_8_UV and M-TrPE-MC_8_UV films, as expected, EL spectra

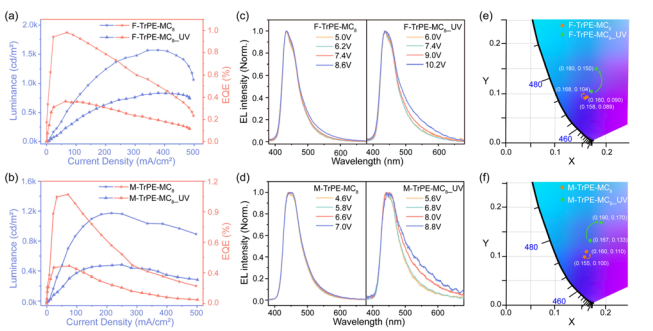

Fig. 4 Device performance of F-TrPE-MC_8 and M-TrPE-MC_8-based OLEDs. Luminance–current density characteristics and maximum external quantum efficiency (EQE) *versus* current density curves for F-TrPE-MC_8 (a), M-TrPE-MC_8 (b)-based OLEDs devices. Electroluminescence (EL) spectra of devices based on F-TrPE-MC_8 (b), M-TrPE-MC_8 (d) pristine film and aged film in the atmosphere, together with their corresponding CIE (e and f), the arrow points into the CIE of increasing current density.

Table 2 Performance of the OLED based on F-TrPE-MC_8, M-TrPE-MC_8, F-TrPE-MC_8_UV and M-TrPE-MC_8_UV films

Emissive layer	EL (nm)	V_{on} (V)	L_{max} (cd m^{-2})	EQE (%)	CIE	
					$L_{turn\ on}$	L_{max}
F-TrPE-MC_8	436/450	4.4	1570.0	0.98	(0.158, 0.089)	(0.160, 0.090)
F-TrPE-MC_8-UV	436/450	5.8	834.8	0.36	(0.168, 0.104)	(0.180, 0.150)
M-TrPE-MC_8	440/455	4.2	1175.4	1.10	(0.155, 0.100)	(0.160, 0.110)
M-TrPE-MC_8-UV	440/455	5.2	489.45	0.42	(0.167, 0.133)	(0.190, 0.170)

consisted of two emission peaks at 436 and 450 nm as well as 440 and 455 nm, with a long tail to 650 nm. Commission International de L'Eclairage (CIE) coordinates of the initial EL spectra for devices with irradiation were about (0.167, 0.104) and (0.168, 0.133). However, with increasing applied voltage and current density, undesirable green-band emission at 500 nm ~650 nm appeared, which indicated a relatively weak emission stability, resulting in a low color purity of deep-blue emission (CIE: change to (0.180, 0.150) and (0.190, 0.170)). F-TrPE-MC_8 and M-TrPE-MC_8 pristine spin-coated films are prepared without the effect of the light excitation and O_2, which are act as emissive layer for OLEDs. Interestingly, EL spectra of their devices exhibit two maximum and shoulder emission peaks at about 436 and 450 nm as well as 440 and 455 nm for F-TrPE-MC_8 and M-TrPE-MC_8, respectively, resembling the corresponding PL spectra, as shown in Fig. 1a, 4c and Table 2. More importantly, there are no obvious green-band emission, further confirming no obvious intermolecular aggregation and electron coupling. The corresponding CIE coordinates were about (0.158, 0.089) and (0.155, 0.100), respectively, suggesting a robust deep-blue emission. With the increase in current density from 50 to 400 mA cm^{-2}, stable EL spectra and CIE coordinates ((0.160, 0.090) and (0.160, 0.110)) of F-TrPE-MC_8 devices suggest more stability and color purity of deep-blue emission *versus* M-TrPE-MC_8 devices. Therefore, to suppress the formation of organic radical, LCMs are used to enhance the spectral stability and color stability of deep-blue OLEDs.

In general, the formation of organic radicals is harmful to the device performance. As demonstrated in Fig. S17 (ESI†), it can be observed that the turn-on voltages (V_{on}) of the devices based on F-TrPE-MC_8, M-TrPE-MC_8, F-TrPE-MC_8_UV and M-TrPE-MC_8_UV films are calculated at about 4.4 V, 4.2 V, 5.8 V and 5.2 V, respectively. The corresponding devices based on the F-TrPE-MC_8 and M-TrPE-MC_8 pristine films exhibited a maximum brightness of 1570 cd m^{-2} (obtained at 377.6 mA cm^{-2}, 7.2 V) and 1175 cd m^{-2} (obtained at 215.4 mA cm^{-2}, 5.8 V), respectively; the maximum external quantum efficiency (EQE) of 0.98% and 1.1% was recorded with a driving current density of 68.7 and 70.7 mA cm^{-2}, respectively. The performance of the devices is comparable to the conventional solution-processed deep-blue OLEDs. However, if the F-TrPE-MC_8_UV and M-TrPE-MC_8_UV aged films were selected as the emissive layer, the maximum luminance density was about 834.8 cd m^{-2} (recorded at 378.6 mA cm^{-2}, 8.8 V) and 489.45 cd m^{-2} (recorded at 249.5 mA cm^{-2}, 7 V), respectively. The corresponding maximum EQE values were reduced to 0.36% and 0.42%, respectively. Obviously, OLEDs based on fresh films present a better performance and spectral stability than those of aged film obtained after light excitation, which include color purity, EQE, V_{on} and brightness, confirming the importance of the suppression of organic radical in OLEDs.

Conclusions

In summary, the effects of organic radicals in LCMs on their photophysical property are systematically investigated toward fabricating stable deep-blue OLEDs. Owing to the intramolecular excitonic behavior induced by large steric units, model F-TrPE-MC_8 and M-TrPE-MC_8 present a robust deep-blue emission with extremely high emission efficiency of nearly 80%. However, unsaturated bonds in model F-TrPE-MC_8 and M-TrPE-MC_8 are easily sensitized by the light and oxygen, resulting in the formation of organic radicals. These radicals act as defect structure to trap and quench singlet exciton, which may reduce efficiency and color purity of deep-blue emission. Moreover, from the ultrafast photophysical dynamic analysis, compared to the pristine spin-coated ones, singlet exciton had a short decay time in aged film (under the light and oxygen). Therefore, compared to aged film, OLEDs based on the fresh films had a more stable deep-blue emission with a CIE of (0.16, 0.09), better device performance (2.5 folds) and high brightness (2 folds) at low current density. Thus, to avoid the formation of this radical in common, LCMs is preconditioned to obtain high performance and stable deep-blue OLEDs.

Conflicts of interest

There are no conflicts to declare.

Acknowledgements

This work is financially supported by followed projects: W. Huang, J. Lin, and Y. Han acknowledge support from the National Natural Science Foundation of China (No. 62288102, 61874053, 22075136, and 62205141); J. Lin also thanks the support from the Natural Science Foundation of Jiangsu Province (No. BK20200700); Y. Han thanks the support from China Postdoctoral Science Foundation (No. 2022M711591) and Jiangsu Funding Program for Excellent Postdoctoral Talent. This project has also received the open research fund from the State Key Laboratory of Luminescent Materials and Devices (South China University of Technology).

Notes and references

1 J. H. Burroughes, D. D. C. Bradley, A. R. Brown, R. N. Marks, K. Mackay, R. H. Friend, P. L. Burns and A. B. Holmes, Light-emitting diodes based on conjugated polymers, *Nature*, 1990, **347**(6293), 539–541.
2 A. T. Haedler, K. Klaus, I. Abey, W. Bernd, K. Milan, H. Natalie, K. H. Jürgen, S. Hans-Werner and H. Richard, Long-range energy transport in single supramolecular nanofibres at room temperature, *Nature*, 2015, **523**(7559), 196–199.
3 X. Guo and A. Facchetti, The journey of conducting polymers from discovery to application, *Nat. Mater.*, 2020, **19**(9), 922–928.
4 J. Ouyang, Application of intrinsically conducting polymers in flexible electronics, *SmartMat*, 2021, **2**(3), 263–285.
5 L. Tu, Y. Xie, Z. Li and B. Tang, Aggregation-induced emission: Red and near-infrared organic light-emitting diodes, *SmartMat*, 2021, **2**(3), 326–346.
6 Y. Zhao, L. Liu, F. Zhang, C.-A. Di and D. Zhu, Advances in organic thermoelectric materials and devices for smart applications, *SmartMat*, 2021, **2**(4), 426–445.
7 J. Lin, B. Liu, M. Yu, X. Wang, Z. Lin, X. Zhang, C. Sun, J. Cabanillas-Gonzalez, L. Xie, F. Liu, C. Ou, L. Bai, Y. Han, M. Xu, W. Zhu, T. A. Smith, P. N. Stavrinou, D. D. C. Bradley and W. Huang, Ultrastable Supramolecular Self-Encapsulated Wide-Bandgap Conjugated Polymers for Large-Area and Flexible Electroluminescent Devices, *Adv. Mater.*, 2019, **31**(1), 1804811.
8 F. C. Spano and C. Silva, H- and J-Aggregate Behavior in Polymeric Semiconductors, *Annu. Rev. Phys. Chem.*, 2014, **65**(1), 477–500.
9 M. Gaal, E. J. W. List and U. Scherf, Excimers or Emissive On-Chain Defects?, *Macromolecules*, 2003, **36**(11), 4236–4237.
10 J. S. Kim and T. M. Swager, Control of conformational and interpolymer effects in conjugated polymers, *Nature*, 2001, **411**(6841), 1030–1034.
11 T. Ye, J. Chen and D. Ma, Electroluminescence of poly (*N*-vinylcarbazole) films: fluorescence, phosphorescence and electromers, *Phys. Chem. Chem. Phys.*, 2010, **12**(47), 15410–15413.
12 L. H. Xie, C. R. Yin, W. Y. Lai, Q. L. Fan and W. Huang, Polyfluorene-based semiconductors combined with various periodic table elements for organic electronics, *Prog. Polym. Sci.*, 2012, **37**(9), 1192–1264.
13 M.-N. Yu, J.-Y. Lin, Y.-X. Li, H. Soleimaninejad, C.-J. Ou, L.-B. Bai, B. Liu, W. Liu, Q. Wei, Y.-F. Bo, T. A. Smith, D. E. Dunstan, K. P. Ghiggino, L.-H. Xie, C.-X. Xu, D. D. C. Bradley and W. Huang, Emission Enhanced and Stabilized by Stereoisomeric Strategy in Hierarchical Uniform Supramolecular Framework, *Chem*, 2019, **5**(9), 2470–2483.
14 C. Ou, N. J. Cheetham, J. Weng, M. Yu, J. Lin, X. Wang, C. Sun, J. Cabanillas-Gonzalez, L. Xie, L. Bai, Y. Han, D. D. C. Bradley and W. Huang, Hierarchical Uniform Supramolecular Conjugated Spherulites with Suppression of Defect Emission, *iScience*, 2019, **16**, 399–409.
15 F. Cacialli, J. S. Wilson, J. J. Michels, C. Daniel, C. Silva, R. H. Friend, N. Severin, P. Samorì, J. P. Rabe, M. J. O'Connell, P. N. Taylor and H. L. Anderson, Cyclodextrin-threaded conjugated polyrotaxanes as insulated molecular wires with reduced interstrand interactions, *Nat. Mater.*, 2002, **1**(3), 160–164.
16 D. Wang, C. Cheng, T. Tsuboi and Q. Zhang, Degradation mechanisms in blue organic light-emitting diodes, *CCS Chem.*, 2020, **2**(4), 1278–1296.
17 B. H. Cumpston and K. F. Jensen, Photo-oxidation of polymers used in electroluminescent devices, *Synth. Met.*, 1995, **73**(3), 195–199.
18 S. Scholz, D. Kondakov, B. Lüssem and K. Leo, Degradation Mechanisms and Reactions in Organic Light-Emitting Devices, *Chem. Rev.*, 2015, **115**(16), 8449.
19 S. Y. Cho, A. C. Grimsdale, D. J. Jones, S. E. Watkins and A. B. Holmes, Polyfluorenes without monoalkylfluorene defects, *J. Am. Chem. Soc.*, 2007, **129**(39), 11910–11911.
20 H. Heil, G. Andress, R. Schmechel, H. Von Seggern, J. Steiger, K. Bonrad and R. Sprengard, Sunlight stability of organic light-emitting diodes, *J. Appl. Phys.*, 2005, **97**(12), 124501.
21 W. Qi, Y. Luo and H. Aziz, Evidence of intermolecular species formation with electrical aging in anthracene-based blue organic light-emitting devices, *J. Appl. Phys.*, 2010, **107**(8), 913–1067.
22 B. Cumpston, I. Parker and K. Jensen, In situ characterization of the oxidative degradation of a polymeric light emitting device, *J. Appl. Phys.*, 1997, **81**(8), 3716–3720.
23 S. Schmidbauer, A. Hohenleutner and B. König, Chemical Degradation in Organic Light-Emitting Devices: Mechanisms and Implications for the Design of New Materials, *Adv. Mater.*, 2013, **25**(15), 2114–2129.
24 D. Y. Kondakov, T. D. Pawlik, W. F. Nichols and W. C. Lenhart, Free-radical pathways in operational degradation of OLEDs, *J. Soc. Inf. Disp.*, 2008, **16**(1), 37–46.
25 N. Dam, R. D. Scurlock, B. Wang, L. Ma, M. Sundahl and P. R. Ogilby, Singlet oxygen as a reactive intermediate in the photodegradation of phenylenevinylene oligomers, *Chem. Mater.*, 1999, **11**(5), 1302–1305.
26 R. D. Scurlock, B. Wang, P. R. Ogilby, J. R. Sheats and R. L. Clough, Singlet oxygen as a reactive intermediate in the photodegradation of an electroluminescent polymer, *J. Am. Chem. Soc.*, 1995, **117**(41), 10194–10202.
27 Z. Chen, Y. Li and F. Huang, Persistent and stable organic radicals: Design, synthesis, and applications, *Chem*, 2021, **7**(2), 288–332.
28 Z. Chen, W. Li, M. A. Sabuj, Y. Li, W. Zhu, M. Zeng, C. S. Sarap, M. M. Huda, X. Qiao, X. Peng, D. Ma, Y. Ma, N. Rai and F. Huang, Evolution of the electronic structure in open-shell donor-acceptor organic semiconductors, *Nat. Commun.*, 2021, **12**(1), 5889.
29 R. H. Young, C. W. Tang and A. P. Marchetti, Current-induced fluorescence quenching in organic light-emitting diodes, *Appl. Phys. Lett.*, 2002, **80**(5), 874–876.
30 C. Zhao and L. Duan, Review on photo- and electrical aging mechanisms for neutral excitons and ions in organic light-emitting diodes, *J. Mater. Chem. C*, 2020, **8**(3), 803–820.

31 A. J. Heeger, Semiconducting polymers: the Third Generation, *Chem. Soc. Rev.*, 2010, **39**(7), 2354–2371.
32 S. Bandyopadhyay, S. Kundu, A. Giri and A. Patra, A smart photosensitizer based on a red emitting solution processable porous polymer: generation of reactive oxygen species, *Chem. Commun.*, 2018, **54**(66), 9123–9126.
33 S. Ma, Y. Liu, J. Zhang, B. Xu and W. Tian, Polymorphism-dependent enhanced emission in molecular aggregates: J-aggregate versus X-aggregate, *J. Phys. Chem. Lett.*, 2020, **11**(24), 10504–10510.
34 L. Wang, T. Yu, Z. Xie, X. Chen, Z. Yang, Y. Zhang, M. P. Aldred and Z. Chi, Design, synthesis and photochromism studies of thienyl containing triarylethylene derivatives and their applications in real-time photoresponsive surfaces, *J. Mater. Chem. C*, 2018, **6**(32), 8832–8838.
35 L. Wang, T. Yu, Z. Xie, E. Ubba, T. Zhan, Z. Yang, Y. Zhang and Z. Chi, Gated photochromic molecules with AIEgen: turn-on the photochromism with an oxidation reagent, *RSC Adv.*, 2018, **8**(33), 18613–18618.
36 J.-Y. Lin, W.-S. Zhu, F. Liu, L.-H. Xie, L. Zhang, R. Xia, G.-C. Xing and W. Huang, A Rational Molecular Design of β-Phase Polydiarylfluorenes: Synthesis, Morphology, and Organic Lasers, *Macromolecules*, 2014, **47**(3), 1001–1007.
37 C.-J. Ou, C. Zhu, X.-H. Ding, L. Yang, J.-Y. Lin, L.-H. Xie, Y. Qian, C.-X. Xu, J.-F. Zhao and W. Huang, Dimerization effect of fluorene-based semiconductors on conformational planarization for microcrystal lasing, *J. Mater. Chem. C*, 2017, **5**(22), 5345–5355.
38 Y.-M. Han, L.-B. Bai, C.-R. Yin, C.-J. Ou, X.-W. Zhang, Z.-Y. Zuo, B. Liu, M.-N. Yu, J.-Y. Lin, J.-F. Zhao, W.-S. Zhu, Y.-Y. Liu, J.-W. Li, J.-P. Wang, L.-H. Xie and W. Huang, Solution-processed diarylfluorene derivatives for violet-blue amplified spontaneous emission and electroluminescence, *J. Mater. Chem. C*, 2017, **5**(38), 9903–9910.
39 C. Pan, K. Sugiyasu, Y. Wakayama, A. Sato and M. Takeuchi, Thermoplastic Fluorescent Conjugated Polymers: Benefits of Preventing π–π Stacking, *Angew. Chem., Int. Ed.*, 2013, **52**(41), 10775–10779.
40 Y. Yamakoshi, N. Umezawa, A. Ryu, K. Arakane, N. Miyata, Y. Goda, T. Masumizu and T. Nagano, Active oxygen species generated from photoexcited fullerene (C60) as potential medicines: O2-* versus 1O2, *J. Am. Chem. Soc.*, 2003, **125**(42), 12803–12809.
41 G. Veréb, L. Manczinger, G. Bozsó, A. Sienkiewicz, L. Forró, K. Mogyorósi, K. Hernádi and A. Dombi, Comparison of the photocatalytic efficiencies of bare and doped rutile and anatase TiO2 photocatalysts under visible light for phenol degradation and E. coli inactivation, *Appl. Catal., B*, 2013, **129**, 566–574.
42 L. Gao, B. Zhou, F. Wang, R. Yuan, H. Chen and X. Han, Effect of dissolved organic matters and inorganic ions on TiO2 photocatalysis of diclofenac: mechanistic study and degradation pathways, *Environ. Sci. Pollut. Res.*, 2020, **27**(2), 2044–2053.
43 Z. Wang, W. Ma, C. Chen, H. Ji and J. Zhao, Probing paramagnetic species in titania-based heterogeneous photocatalysis by electron spin resonance (ESR) spectroscopy—A mini review, *Chem. Eng. J.*, 2011, **170**(2–3), 353–362.
44 H. Y. Chung, D. W. Kim, J.-M. Park, J. Oh, D. Kim and S. Y. Park, Femtosecond Transient Absorption Studies of Polymer Aggregation on Photovoltaic Performance: Role of an Integrated Aggregation Promotor in the Polymer Chain, *J. Phys. Chem. C*, 2021, **125**(14), 7568–7580.